Dynamic Regulation of SARS-CoV-2 Binding and Cell Entry Mechanisms in Remodeled Human Ventricular Myocardium

Michael R. Bristow, MD, PhD;, Lawrence S. Zisman, MD;, Natasha L. Altman, MD;, Edward M. Gilbert, MD;, Brian D. Lowes, MD, PhD;, Wayne A. Minobe, BS;, Dobromir Slavov, PhD;, Jessica A. Schwisow, BS;, Erin M. Rodriguez, BA;, Ian A. Carroll, PhD;, Thomas A. Keuer, MS;, Peter M. Buttrick, MD;, David P. Kao, MD.

PII: S2452-302X(20)30264-3

DOI: https://doi.org/10.1016/j.jacbts.2020.06.007

Reference: JACBTS 483

To appear in: *JACC: Basic to Translational Science*

Received Date: 5 May 2020

Revised Date: 17 June 2020

Accepted Date: 17 June 2020

Please cite this article as: Bristow MR, Zisman LS, Altman NL, Gilbert EM, Lowes BD, Minobe WA, Slavov D, Schwisow JA, Rodriguez EM, Carroll IA, Keuer TA, Buttrick PM, Kao DP, Dynamic Regulation of SARS-CoV-2 Binding and Cell Entry Mechanisms in Remodeled Human Ventricular Myocardium, *JACC: Basic to Translational Science* (2020), doi: https://doi.org/10.1016/j.jacbts.2020.06.007.

Dynamic Regulation of SARS-CoV-2 Binding and Cell Entry Mechanisms in Remodeled Human Ventricular Myocardium

Michael R. Bristow, MD, PhD;[1,2,3] Lawrence S. Zisman, MD;[4] Natasha L. Altman, MD;[1,3] Edward M. Gilbert, MD;[5] Brian D. Lowes, MD, PhD;[6] Wayne A. Minobe, BS;[1] Dobromir Slavov, PhD;[1] Jessica A. Schwisow, BS;[1] Erin M. Rodriguez, BA;[1] Ian A. Carroll, PhD;[1,2] Thomas A. Keuer, MS;[2] Peter M. Buttrick, MD;[1,3] David P. Kao, MD.[1,3]

[1]Division of Cardiology, University of Colorado, Denver/Anschutz Medical Campus, Aurora, Colorado, United States of America
[2]ARCA biopharma, Westminster, Colorado, United States of America
[3]University of Colorado Cardiovascular Institute Pharmacogenomics, Boulder and Aurora, Colorado, United States of America
[4]Gossamer Bio, San Diego, CA, United States of America
[5]Division of Cardiology, University of Utah Medical Center, Salt Lake City, Utah, United States of America
[6]Division of Cardiology, University of Nebraska Medical Center, Omaha, Nebraska, United States of America

Corresponding author: Michael R. Bristow MD, PhD; B-139 Research 2, 12700 E. 19th Ave, Aurora, CO 80045; michael.bristow@cuanschutz.edu

Acknowledgements

The authors thank Rachel Rosenberg, MS, MBA and Laura Hofstatter for manuscript proofing and handling.

No author has any conflict of interest with any aspect of the data or its interpretation.

This work was supported by NHLBI grants 2R01 HL48913 (awarded to MRB), 1R01 HL71118 (awarded to MRB and BDL), K23 HL068875 (awarded to BDL), K08 HL125725 (awarded to DPK), AHA grant 16SFRN31420008 (awarded to PMB and MRB), and an AHA COVID-19 Rapid Response grant awarded to MRB.

Highlights

1. The SARS-CoV-2 cellular receptor ACE2 and 5 proteases implicated in fusion of virus and cell membranes that are vital to cell entry were expressed at the mRNA level in RNA extracted from septal endomyocardial biopsies of F/NDC and nonfailing (NF) control patients.
2. ACE 2 was upregulated by 1.97 fold in 46 F/NDC patients compared to NF, but proteases showed similar degrees of expression.
3. On LV reverse remodeling effected by beta-blocking agents, ACE2 expression, in the presence of unchanged doses of ACE inhibitors or ARBs, downregulated into the normal range.
4. ITGA5, an integrin that binds to ACE2 and to a motif in the CoV-2 spike protein binding domain, was expressed in both NF and F/NDC, upregulated in the latter at baseline and decreased in expression on reverse remodeling similar to ACE2, and is a candidate for facilitating CoV-2 binding and cell entry in LV myocardium.

SUMMARY

Using serial analysis of myocardial gene expression employing endomyocardial biopsy starting material in a dilated cardiomyopathy cohort, we show that the SARS-CoV-2 cardiac myocyte receptor ACE2 is upregulated with remodeling and with reverse remodeling down-regulates into the normal range. The proteases responsible for virus-cell membrane fusion were expressed but not regulated with remodeling. In addition, a new candidate for CoV-2 cell binding and entry was identified, the integrin ITGA5. The upregulation in ACE2 in remodeled LVs may explain worse outcomes in COVID-19 patients with underlying myocardial disorders, and counteracting ACE2 upregulation is a possible therapeutic approach to minimizing cardiac damage.

ABBREVIATIONS

Term	Definition
COVID-19	Infection with the SARS-CoV-2 virus, or the virus itself
CoV-2	The SARS-CoV-2 virus
ACE2	Angiotensin converting enzyme 2
ACE	Angiotensin converting enzyme
F/NDC	Nonischemic dilated cardiomyopathy with heart failure
HFrEF	Heart failure with reduced (<0.50) left ventricular ejection fraction
LOCF	Last observation carried forward
EmBx	Endomyocardial biopsy
RNA-Seq	RNA sequencing
ITGA5	Integrin A5

RAS	Renin angiotensin system
RAAS	Renin angiotensin aldosterone system

KEY WORDS: COVID-19, ACE2, Proteases, Integrins, Ventricular remodeling

INTRODUCTION

The 2020 COVID-19 pandemic has many unique clinical features, including high infectivity, a protean clinical presentation and course, and life-threatening potential (1). Myocardial involvement is an important pathophysiologic component of some critically ill patients with SARS-CoV-2 (CoV-2) infections (2,6), either due to myocarditis (5,6) or myocardial dysfunction without evidence of inflammation (2-4). The prevalence of cardiac complications in patients without underlying heart disease ranges from 20-30% (7-9), which when present worsens prognosis. In the initial report of patients receiving intensive care, evidence of cardiac injury was associated with a 50% mortality compared to <10% without such evidence (3). The prognosis worsens further when evidence of myocardial injury is superimposed on pre-existing cardiovascular disease, with mortality rising to above 60% (3).

A well-established pathway by which the CoV-2 virus gains entry into cells includes membrane attachment by binding to angiotensin converting enzyme 2 (ACE2) (10,11), fusion of viral and cell surface membranes through the recruitment of host proteases (12-14), and virus internalization followed by assembly of cytoplasmic membranous structures into replication vesicles (15). In addition, there are other possible mechanisms of virus internalization such as binding to integrins (16,17), some of which also bind to ACE2 (18,19). Although CoV-2-cell internalization has been investigated in model systems (10-15) and is beginning to be evaluated in the human heart (20) it is unclear if the virus enters human cardiac myocytes, and if the necessary biologic constituents are expressed in the heart. Of particular importance is the role of ACE2; in human ventricular myocardium ACE2 is a highly functional enzyme present in cardiac myocytes (20) that breaks down angiotensin II (ANG II) to the counter-regulatory peptide angiotensin-(1-7) (21,22). In explanted human heart preparations from patients with end stage reduced ejection fraction heart failure (HFrEF), ACE2 enzyme activity (22) as well as gene expression at the mRNA (20,23) and protein (20,22) levels are upregulated compared to organ donor controls. This is potentially important because upregulated ACE2 might be a

mechanism by which CoV-2 myocardial involvement is more prominent in patients with underlying heart muscle disease (20).

However, it is unclear if ACE2 is upregulated in intact hearts with less severe pathologic remodeling/dysfunction than in explanted hearts from cardiac transplant recipients, who in contrast to most organ donor controls have been treated with renin-angiotensin (RAS) system inhibitors (24,25). In addition, it is not clear if the proteases that prime and facilitate membrane fusion are expressed or regulated in the remodeled, failing human heart. Finally, there is limited information on the status of integrins, particularly those that can bind to ACE2 or to the CoV-2 virus itself, to potentially effect virus-cell internalization (16). In order to obtain information on these mechanisms in nonfailing and remodeled intact human heart we analyzed data from a serial analysis of myocardial gene expression cohort study (26), where reverse remodeled LVs were compared to unchanged ventricles exposed to the same pharmacologic regimen, with each subject serving as their own control.

METHODS

Patient material and protocol

Control subjects were four individuals with LVEFs ≥50% (mean ± SD of 59±7%) who had endomyocardial biopsies to rule out myocarditis or other infiltrative processes, and had no histopathologic abnormalities. Heart failure patients with reduced LVEF (HFrEF) and pathologic eccentric remodeling consisted of 47 patients with LVEFs ≤40% and NYHA Class II or III heart failure from nonischemic dilated cardiomyopathy (F/NDC) of uncertain etiology. These patients had RV mid-distal interventricular septum endomyocardial biopsies (EmBx) performed at baseline for diagnostic and research purposes, and then after 3 and 12 months of beta-blocker therapy for research material only, as previously described (26,27) (NCT01798992). The 4 subjects with normal LV function and 46 of the 47 NDC patients (mean LVEF 26.6±8.7%) had technically adequate global gene expression measurements by microarray in extracted RNA, as

previously described (26). Beta-blockers were initiated and uptitrated to target doses (26,27), reaching mean doses at the last EmBx and EF measurements of 75±17 mg/d for 16 carvedilol, and 169±55 mg/d for 30 metoprolol succinate treated patients. The clinical study was designed to detect differences in gene expression mediated through blockade of individual β_1-, α_{1A}- and β_2-adrenregic receptors (ARs), but no systematic changes between treatment groups were detected (27) and the three groups, who had in common blockade of β_1-ARs, were combined into one cohort.

Eight patients had only a 3 month EmBx (1 sudden cardiac death, 1 LVAD placement, 1 traumatic injury unrelated to the study that precluded compliance with the protocol, 6 withdrawals before 12 months), and their results were grouped with the 12 month studies in a last observation carried forward (LOCF) analysis. In these 8 LOCF subjects the degree of reverse remodeling was not statistically significantly different from patients with 12 month measurements (respective improvements in LVEF of 16±5 absolute % vs. 22±4 %, P = 0.28). In addition to microarray global gene expression was also measured by RNA-sequencing (RNA-Seq), in 6 "Super-responders" with LVEF increases of ≥10 absolute % compared to 6 gender and age matched subjects with LVEF increases of <5 absolute % (Supplement, Table S1) (26,28). LVEF was measured by radionuclide SPECT imaging as previously described (27,29), and a reverse remodeling Responder in the entire 46 patient F/NDC cohort was defined as an LOCF increase in LVEF of ≥5 absolute % at 3 months or ≥8% at 12 months (26,27). Nonresponders were subjects who did not meet these LVEF change criteria. EmBx and right heart catheterization were performed as previously described (26,27), and there were no procedure-related complications.

All patients signed written consent for this multi-center study conducted at the University of Colorado Anschutz Medical Campus and the University of Utah Medical Center. The study

included a Data and Safety Monitoring Board and was approved by the Institutional Review Boards at both sites.

RNA extraction and mRNA expression measurements

RNA extraction was performed as previously described (26,27). All individual patient mRNA measurements were from the same RNA extraction, typically involving 2-5 separate EmBx samples per study. Extracted RNA was stored at -80°C until use, and microarray and RNA-Seq methodologies were as previously described (26). Microarray gene expression data were normalized by log-scale robust multi-microarray analysis to yield output in fluorescence intensity on an exponential scale. RNA-Seq data transcript levels were quantified as fragments per kilobase of exon per million mapped reads, as previously described (26). Fold change or fold difference was calculated by log2 transformation as described (26).

Data analysis and statistical tests

We used both baseline comparisons between NF controls and F/NDC plus changes from baseline in F/NDC patients to construct an ordered classification of four degrees of remodeling association (Supplement, Table S2). For baseline studies, where only microarray data were available, alpha was set at <0.05. As described in the Supplement (Table S2), in serially evaluated N/NDC patients these results were then linked to the reverse remodeling mRNA results measured by both the microarray and RNA-Seq platforms. The estimated alpha levels based on achieving P <0.05 in more than one condition including directionality requirements are given in the Supplement (Table S2): *unequivocal evidence,* 0.0001; *evidence*, 0.002; and *possible evidence*, 0.08. The statistical significance of all gene expression data was analyzed in the same way, by non-parametric methods using Wilcoxon rank sum or signed rank tests. Correlation analysis was by Spearman's Rho LVEF data for which evidence of non-normal distribution was absent (26), and baseline characteristics were analyzed by t-tests or contingency table analysis.

Because several analyzed gene expression groups had small Ns (NF, 4; RNA-Seq 6 R and 6 NR; LOCF 3 month F/NDC, 5 Rs and 3NRs) we used means and standard deviations (SD) or for change values standard errors of the mean (SEM) as estimates of central tendency and dispersion, in both the small N groups and larger groups to which these data were compared. For microarray data (30 R and 16 NR) group size was sufficient for data to be also presented as medians and 25%, 75% interquartile ranges. Thus in gene expression analyses conducted exclusively in groups where sample sizes were >6 nonparametric statistics and median, IQR data are presented, but when smaller gene expression group sizes were analyzed or compared nonparametric significance tests plus means and SDs or SEMs are used.

R, GraphPad Prism and XLSTAT/Excel were the statistical software packages used.

RESULTS

Baseline characteristics

Baseline characteristics for the 46 F/NDC subjects and 4 NF controls are given in Table 1. At baseline the F/NDC and NF characteristics were similar, except for measurements and biomarkers of ventricular dysfunction/remodeling. In F/NDC patients LVEF was more reduced than RVEF (Table 1, Figure 1A), but both were $P < 0.05$ vs. NF. Right heart catheterization data trended abnormal in F/NDC but no measurement was $P < 0.05$ vs. NF. NPPB was elevated in F/NDC compared to NF ($P = 0.035$), but norepinephrine was not significantly different ($P = 0.44$). These data describe a relatively young (mean age 45.6±13.2 years), well compensated HFrEF population with moderate LV dysfunction/remodeling (LVEF 27.2±9.0 %, LV end diastolic volume 232±93 ml). The baseline characteristics of the Responder and Nonresponder groups are also given in Table S3. A markedly greater duration of heart failure in Nonresponders (55.7±67.0 months vs. 7.0±10 months in Responders, $P = 0.011$) was the only difference.

The protocol mandated ACE inhibitor background therapy, and diuretics as needed. Spironolactone was administered as tolerated, and an angiotensin blocking agent (ARB) could

be substituted in ACEI intolerant patients. Table 1 gives the ACEI and ARB doses in enalapril and losartan equivalents (30), at both baseline and the average dose during the 12 month study. All 4 of the NF controls were on ACEIs for suspected and ultimately unproved heart muscle disease, and 44 of the 46 patients were on an ACEI at baseline. There is no difference in ACEI mg dose between F/NDC and NF patients, and no difference between reverse remodeling Responders and Nonresponders in average dose of ACEIs or ARBs.

Reverse remodeling as measured by LVEF and RV over 3 or 12 months

Figure 1B plots baseline, LOCF (8 patients at 3 months and 38 at 12 months), and the LOCF - baseline change for both LVEF and RVEF, by Responder/Nonresponder groups in the F/NDC cohort. For Responders vs. Nonresponders, there is a marked increase in LVEF (by 21.2±1.8 (SEM) absolute % vs. 0.9±0.8% (P <0.0001)), and a lesser, nonsignificant increase in RVEF (respectively 9.4±2.1 % vs. 4.9±3.1 %, P = 0.24). Remodeling data for the selected Super-Responder subcohort and controls are in the Supplement (Table S1), and follow the same pattern, except that the LVEF change from baseline was larger than in the entire cohort (30.7±4.2% vs. 21.2±1.8%, P = 0.035).

Baseline changes in mRNA expression in nonischemic dilated cardiomyopathy patients vs. nonfailing controls

ACE2, other RAS and proteases

Figure 2 contains F/NDC vs. NF baseline mRNA abundance data, for ACE2, two associated RAS genes (AGT and ACE), and five proteases that have been implicated in SARs-CoV or CoV-2-cell membrane priming and fusion (12-14;31-33). Compared to NF controls, ACE2 is substantially upregulated in F/NDC, by 1.97 fold (P = 0.008). ACE expression is unchanged from control, as is angiotensinogen (AGT). The ANG II type 1 and type 2 receptors (AGTR1, AGTR2) are plotted in Figure 3 and are not different between NF and F/NDC. None of the proteases shown in Figure 2 exhibit differences in mRNA expression in F/NDC vs. NF, and only

one (downregulation of cathepsin L-like gene 3 (CTSLL3)) of 11 additional proteases (Supplement, Table S3) exhibited any change in the F/NDC group.

Remodeling-associated genes

At baseline NPPB, PLN and ATP2A2 exhibited changes similar to those in previously reported RT-PCR data (27). NPPB was upregulated by 8.8 fold in F/NDC, and its expression vs. ACE2 was significantly related (Spearman's Rho = 0.73, P <0.0001). Unlike in previous studies using RT-PCR (26,27,34,35) MYH6 was unchanged between NF and F/NDC but was markedly upregulated on reverse remodeling (Table 2) consistent with previously reported data (26,27,35).

Integrins

Table 3 contains NF vs. F/NDC baseline data for 10 integrins previously reported to bind to ACE2 (18,19), facilitate viral internalization (17) or be associated with LV remodeling (36) or cardiac myocyte injury protection (37). Only one, the laminin binding integrin ITGA7, has not been reported to be involved in pathogenic virus cell internalization. Five integrins in Table 3 bind to the RGD motif, recently identified in the CoV-2 spike protein binding domain (16) and used by multiple viruses for binding to integrins. Of the ACE2 binding integrins, ITGA5 expression was 1.28 fold higher in F/NDC compared to NF (P = 0.039) while ITGB1 and ITGA2 were not different. ITGA5 has also been associated with virus internalization (17) and LV remodeling where it decreases with LVAD treatment (36). Of the six non-ACE2 binding integrins listed in Table 3 that have been associated with virus internalization, four reached a P <0.05 for differences between F/NDC and NF, two upregulated (ITGB3 and ITGA4) in F/NDC and two downregulated (ITGB6 and ITGA6). For the three genes previously associated with remodeling other than ITGA5, two (ITGA6 and ITGB6) were downregulated in F/NDC consistent with the decreased expression of ITGA6 in human LVs with dilated cardiomyopathies (36), or the upregulation previously reported with LVAD treatment (36). The laminin binding integrin ITGA7 was upregulated in F/NDC.

Changes in mRNA expression on reverse remodeling

ACE2, other RAS and proteases

Changes in Responders or Nonresponder fold changes based on mean values are given in Table 2, while median and IQR values for microarray data are presented in Tables S3 and S4. In microarray measurements, the near twofold upregulated ACE2 at baseline was downregulated as LV remodeling improved, declining to 0.675 fold (an approximate 1.5 fold decrease, P <0.0001). Three other RAS genes (ACE, AGT, AGTR2) and only one of the proteases shown in Table 2 exhibited changed expression on reverse remodeling. The protease that was downregulated in F/NDC (Table S3, CTSLL3) was not changed with reverse remodeling (fold change from baseline 1.03, P = 0.62 (Table S3)). Although in the R vs NR comparison serine protease 1 (PRSS1) was downregulated on reverse remodeling (fold change 0.90, P = 0.042 (Table S3)) the change was related to an upregulation in the NR group rather than a change in Rs. AGTR1 met criteria for *possible evidence* (P <0.08) for an association with remodeling, with R and not NR upregulation on microarray measurements. RNA Seq data exhibited a decrease in ACE2 expression on reverse remodeling (P = 0.004), with a greater fold change of 0.40 fold (approximate 2.5 fold decline) than in microarray data. Thus, ACE2 met criteria for *unequivocal evidence* (P <0.0001) of a remodeling association. RNA-Seq data for all other RAS and protease genes (Tables 2 and S4) were similar to microarray measurements.

Remodeling-associated genes

As expected, these genes generally changed their expression in directions opposite to their baseline levels (Table 2, Table S4). NPPB, a counter-regulatory peptide considered the premier biomarker of pathologically remodeled ventricular myocardium in tissue (27,35) or plasma (38), exhibited expression behavior very similar to ACE2 including an *unequivocal evidence* rating for remodeling association. MYH6, PLN and ADRB1 all had remodeling associated ratings of *evidence* (P <0.002), while ATP2A2 (Serca 2a) rated *possible evidence*.

Integrins

Reverse remodeling changes in integrins are given in Tables 2 and S4. For the P <0.05 baseline changed genes, ITGB3, ITGB6 and ITGA5 had at least one platform showing significant change on reverse remodeling and thus qualified for *evidence* of a remodeling association (Table 3). ITGA4 and ITGA6 expression did not significantly change on reverse remodeling, and their baseline changes therefore qualified as *possible evidence*. For ITGA7, both microarray and RNA-Seq data met criteria for dynamic downregulation of the baseline upregulated expression and a rating of *unequivocal evidence* of a remodeling association, with a pattern identical to ACE2 and NPPB. Thus, of the ten integrins examined five had at least some evidence of an association with remodeling.

DISCUSSION

In patients with mild-moderate F/NDC, myocardial ACE2 gene expression dynamically regulates with LV remodeling independent of RAS inhibitor treatment, and may explain heightened COVID-19 clinical risk associated with underlying heart muscle disorders

Figure 4 illustrates the positioning and role of ACE2 within the renin-angiotensin-aldosterone system. In the human left ventricle this zinc dependent carboxypeptidase catalyzes the conversion of the octapeptide angiotensin II to the counter-regulatory heptapeptide angiotensin-(1-7), with high activity and efficiency (21). ACE2 exerts a very important function in the heart, by reducing levels of angiotensin II as well as by generating a counter-regulatory peptide that activates MAS1 receptor pathway signaling through G_q and multiple downstream events including reducing ERK1/ERK2 MAP kinase activation (39,40). We found that in a setting where RAS inhibitors were not a potentially confounding variable ACE2 was substantially upregulated in intact failing/remodeled ventricular myocardium, confirming and extending previous work in explanted human hearts (20,22,23). From its upregulated expression in F/NDC at baseline, with reverse remodeling ACE2 then downregulated towards control values in measurements by both

mRNA platforms to yield an *unequivocal evidence* rating for remodeling association corresponding to a P value of <0.0001. In the current study the source of starting material was interventricular septum that reflects molecular changes in either the RV (34) or LV (27), and the reverse remodeling changes were mostly confined to the LV. In addition, the mRNA expression of the 42% ACE2 homologous (41) enzyme ACE was not altered at baseline or on reverse remodeling. Angiotensinogen was similarly unchanged in failing/remodeled ventricular myocardium. The behavior of ACE2 gene expression was analogous and substantially related (baseline values Spearman's Rho of 0.73, P <0.0001) to that of NPPB, another counter-regulatory gene whose remodeling association rating was *unequivocal evidence*.

The upregulation of ACE2 in remodeled intact LV myocardium from subjects with only mild-moderate HFrEF indicates that this regulatory change is not confined to end stage disease in patients who have been treated with RAS inhibitors (20,22,23), and suggests that increased expression of ACE2 in remodeled LVs could be the reason why CoV-2 infected patients with underlying heart muscle disorders are at heightened clinical risk (2,3).

Proteases that participate in CoV-2-cellular membrane priming and fusion do not exhibit regulated expression in F/NDC

We also evaluated the expression of five proteases that participate in fusion of viral and cell membranes (12-14,31-33) when triggered by SARS coronavirus binding to ACE2 (42,43). Expression of CTSL1 (13), TMPRSS11D (13,14), ADAM17 (31) and FURIN (32,33) were detected by both microarray and RNA-Seq platforms. In contrast, TMPRSS2 (12-14), recently implicated in CoV-2-membrane fusion in model systems (12), was low abundance as measured by microarray and could not be detected by RNA-Seq. None of these proteases and only one (CTSLL3) of an additional panel of 11 others exhibited differences between NF and F/NDC, and none changed expression in Responders with reverse remodeling. However, this does not

exclude the possibility that protease protein abundance or enzyme activity may have changed with remodeling.

Integrins, particularly ITGA5, are regulated with remodeling and are candidates for CoV-2 binding and cell entry

We considered that integrins could be a potential participant in CoV-2 cell entry, and found *evidence* or *unequivocal evidence* of remodeling-associated up-regulation in five of the ten investigated. ITGA5, which rated *evidence* of an association with remodeling, can bind to ACE2 (19) and an RBD domain in CoV-2 (16), and thus is a candidate for involvement in CoV-2 cell binding and internalization. The only integrin that achieved *unequivocal evidence* of remodeling association was the laminin binding cardiac and skeletal muscle integrin ITGA7, which has not been reported to bind to ACE2 or pathogenic viruses and which, like ACE2 and NPPB, can be viewed in a counter-regulatory context (37). Five of the ten integrins evaluated contained motifs for binding to an RGD domain, common in pathogenic viruses as a means of cell surface binding and virus internalization, and recently identified in CoV-2 (16). Of these, only ITGA5 and ITGB3 were up-regulated, meaning if Cov-2 did utilize RGD-integrin binding for internalization these two monomers might predispose to greater cell entry. However, these integrins do not dimerize with each other (44), and the ITGA5-ITGB1 or ITGAV-ITGB3 protein product heterodimers, both commonly used by pathogenetic viruses for cell entry, would need to be formed. If RGD binding is disregarded (17), the other up-regulated integrin (rated as *possible evidence*) was ITGA4, which also doesn't dimerize with ITGB3 (44). Alternatively, upregulated integrins could affect virus replication in cardiac myocytes via interaction with integrin linked kinase (45), a pseudokinase adaptor molecule known to bind to ITGB1 and ITGB3 (46).

Cardiac myocyte cell entry of CoV-2, yet to be established, is potentially possible based on binding and internalization mechanisms being present in human ventricular myocardium

Despite substantial evidence that myocardial involvement is common and potentially devastating in COVID-19 disease, identification of CoV-2 virus in cardiac myocytes has not been reported. Cardiac findings on autopsy of COVID-19 patients are limited to a single case of severe pulmonary involvement where on tissue examination no myocardial pathologic findings were observed (47), and two pulmonary death cases where post-mortem myocardial needle biopsy findings were deemed likely to be secondary to pre-existing underlying conditions (48). One of the two needle biopsy subjects had a negative tissue block CoV-2 PCR (48). There is thus far only a single case report of an EmBx in a COVID-19 PCR-proven case, in a patient in cardiogenic shock (49). This patient had electron microscopy imaged coronavirus in ventricular myocardial interstitial cells but not in cardiac myocytes, despite evidence of myofibril lysis (49). However, based on remodeling associated upregulation in ACE2 and the demonstration that all other myocardial cell entry constituents exist in human ventricular myocardium, it would be surprising if CoV-2 can't bind to, enter, replicate and damage human cardiac myocytes. Myocytes contribute approximately 70% of tissue volume in the human left ventricle (50), and ACE2 is definitely cardiac myocyte-expressed according to cell marker findings (20), single cell RNA data (51), and the degree of enzyme activity in vivo (21) and in explanted hearts (22).Thus cardiac myocytes appear to be a vulnerable target for CoV-2, and this needs to be addressed by further histopathologic investigation in hearts exhibiting CoV-2 associated myocardial dysfunction.

ACE2 as a potential therapeutic target in CoV-2 infection

As has been noted by others (52), ACE2 and its receptor for the spike protein binding domain are an attractive therapeutic target for treating or preventing CoV-2 infections. ACE2 small molecule inhibitors have been developed (53) and dramatically lower ACE2 activity in failing human LV preparations, at nanomolar concentrations (22). However, ACE2 is an important counter-regulatory enzyme in the heart, responsible for converting angiotensin II to

angiotensin-(1-7) that is antiproliferative, antifibrotic and a vasorelaxant. Based on gene ablation ACE2 is considered an "essential regulator of heart function" (54). It follows that any ACE2 inhibitor would need to block CoV-2 binding without decreasing enzyme activity, which may be possible through Ab inhibition (11) or the use of decoy receptors (55). Another possibility would be to deploy an ACE2 activator such as diminazene (54) if an ACE2- CoV-2 receptor inhibitor diminishes ACE2 activity. However, if any of these approaches are taken it would be important to rule out other mechanisms of CoV-2 cell entry that would be uninhibited, such as virus-integrin binding.

Perspectives (Clinical Competencies/Translational Outlook)

Angiotensin converting enzyme 2 (ACE2), a counter-regulatory enzyme robustly expressed in human left and right ventricles and the major pathway for breaking down angiotensin II into the antihypertrophic, antifibrotic and vasorelaxant peptide angiotensin-(1-7), has been hijacked by SARS coronaviruses as the binding site for initiation of cell entry. We show that ACE2 is upregulated in eccentrically remodeled/failing LVs, and then decreases expression with reverse remodeling. This regulatory behavior was independent of RAS inhibitors as doses of ACEIs or ARBs weren't different in patients that reverse remodeled compared to those that didn't. ACE2's remodeling expression behavior was identical to NPPB, another counter-regulatory gene that leads to generation of the antiproliferative vasodilator peptide BNP. Upregulated ACE2 should be viewed as beneficial to a remodeled, failing heart, although it may increase the risk of CoV-2 cell invasion and cytopathology. It stands that any therapeutic approach involving ACE2 should focus on inhibiting CoV-2 binding, while maintaining enzyme activity.

The data presented are another example of reverse translation, where an enzyme that was originally characterized and shown to be upregulated in failing, pathologically remodeled human hearts was discovered to be the cell transducer for a worldwide pandemic. The precise biologic mechanisms involved in SARS coronavirus cell entry and damage are now being investigated at the basic science level, and therapeutic strategies involving ACE2 inhibition or intervention at downstream events may result in forward translation back to the clinical setting.

REFERENCES

1. Guan WJ, Ni ZY, Liang WH, et al. Clinical characteristics of coronavirus disease 2019 in China [published online ahead of print February 28, 2020]. N Engl J Med. doi:10.1056/NEJMoa2002032.
2. Zhou F, Yu T, Du R, et al. Clinical course and risk factors for mortality of adult inpatients with COVID-19 in Wuhan, China: a retrospective cohort study. Lancet. 2020;395(10229):1054-1062. doi:10.1016/S0140-6736(20)30566-3.
3. Shi S, Qin M, Shen B, et al. Association of cardiac injury with mortality in hospitalized patients with COVID-19 in Wuhan, China [published online ahead of print March 25, 2020]. JAMA Cardiol. doi:10.1001/jamacardio.2020.0950.
4. Ruan Q, Yang K, Wang W, Jiang L, Song J. Clinical predictors of mortality due to COVID-19 based on an analysis of data of 150 patients from Wuhan, China [published online ahead of print, 2020 Mar 3] [published correction appears in Intensive Care Med. 2020 Apr 6]. Intensive Care Med. 2020;1–3. doi:10.1007/s00134-020-05991-x.
5. Inciardi RM, Lupi L, Zaccone G, et al. Cardiac involvement in a patient with coronavirus disease 2019 (COVID-19) [published online ahead of print March 27, 2020]. JAMA Cardiol. doi:10.1001/jamacardio.2020.1096.
6. Hu H, Ma F, Wei X, Fang Y. Coronavirus fulminant myocarditis saved with glucocorticoid and human immunoglobulin [published online ahead of print March 16, 2020]. Eur Heart J. doi:10.1093/eurheartj/eurheartj190.
7. Guo T, Fan Y, Chen M, et al. Cardiovascular implications of fatal outcomes of patients with coronavirus disease 2019 (COVID-19) [published online ahead of print March 27, 2020]. JAMA Cardiol. doi:10.1001/jamacardio.20201017.
8. Zheng YY, Ma YT, Zhang JY, Xie X. COVID-19 and the cardiovascular system. Nat Rev Cardiol. 2020;17(5):259-260. doi:10.1038/s41569-020-0360-5.

9. Lippi G, Lavie CJ, Sanchis-Gomar F. Cardiac troponin I in patients with coronavirus disease 2019 (COVID-19): evidence from a meta-analysis [published online March 10, 2020]. Prog Cardiovasc Dis. doi: 10.1016/j.pcad.2020.03.001.
10. Wrapp D, Wang N, Corbett KS, et al. Cryo-EM structure of the 2019-nCoV spike in the perfusion conformation. Science. 2020; 367(6483):1260-1263. doi:10.1126/science.abb2507.
11. Walls AC, Park YJ, Tortorici MA, Wall A, McGuire AT, Veesler D. Structure, Function, and Antigenicity of the SARS-CoV-2 Spike Glycoprotein. Cell. 2020;181(2):281-292.e6. doi: 10.1016/j.cell.2020.02.058.
12. Hoffmann M, Kleine-Weber H, Schroeder S, et al. SARS-CoV-2 Cell Entry Depends on ACE2 and TMPRSS2 and Is Blocked by a Clinically Proven Protease Inhibitor. Cell. 2020;181(2):271–280.e8. doi:10.1016/j.cell.2020.02.052.
13. Belouzard S, Chu VC, Whittaker GR. Activation of the SARS coronavirus spike protein via sequential proteolytic cleavage at two distinct sites. Proc Natl Acad Sci USA. 2009;106(14):5871-5876. doi: 10.1073/pnas.0809524106.
14. Bertram S, Glowacka I, Mueller MA, et al. Cleavage and activation of the severe acute respiratory syndrome coronavirus spike protein by human airway trypsin-like protease. angiotensin converting enzyme
15. Hagemeijer MC, Rottier PJM, de Haan CAM. Biogenesis and dynamics of the coronavirus replicative structures. Viruses. 2012;4(11):3245-3269. doi:10.3390/v4113245.
16. Sigrist CJA, Bridge A, Le Mercier P. A potential role for integrins in host cell entry by SARS-CoV-2. Antiviral Research. 2020;177:104759. doi:10.1016/j.antiviral.2020.104759.
17. Hussein HA, Walker LR, Abdel-Raouf UM, Desouky SA, Montasser AK, Akula SM. Beyond RGD: virus interactions with integrins. Arch Virol. 2015;160(11):2669-2681. doi:10.1007/s00705-015-2579-8.

18. Lin Q, Keller RS, Weaver B, Zisman LS. Interaction of ACE2 and integrin beta1 in failing human heart. Biochim Biophys Acta. 2004;1689(3):175-178. doi:10.1016/j.bbadis.2004.05.005.

19. Clarke NE, Fisher MJ, Porter KE, Lambert DW, Turner AJ. Angiotensin converting enzyme (ACE) and ACE2 bind integrins and ACE2 regulates integrin signalling. PLoS One. 2012;7(4):e34747. doi:10.1371/journal.pone.0034747.

20. Chen L, Li X, Chen M, Feng Y, Xiong C. The ACE2 expression in human heart indicates new potential mechanism of heart injury among patients infected with SARS-CoV-2 [published online ahead of print March 30, 2020]. Cardiovasc Res. doi:10.1093/cvr/cvaa078.

21. Zisman LS, Meixell GE, Bristow MR, Canver CC. Angiotensin-(1-7) formation in the intact human heart: in vivo dependence on angiotensin II as substrate. Circulation. 2003;108(14):1679-1681. doi:10.1161/01.CIR.0000094733.61689.D4.

22. Zisman LS, Keller RS, Weaver B, et al. Increased angiotensin-(1-7)-forming activity in failing human heart ventricles: evidence for upregulation of the angiotensin-converting enzyme Homologue ACE2. Circulation. 2003;108(14):1707-1712. doi:10.1161/01.CIR.0000094734.67990.99.

23. Goulter AB, Goddard MJ, Allen JC, Clark KL. ACE2 gene expression is up-regulated in the human failing heart. BMC Med. 2004;2:19. doi:10.1186/1741-7015-2-19.

24. Ferrario CM, Jessup J, Chappell MC et al. Effect of angiotensin-converting enzyme inhibition and angiotensin II receptor blockers on cardiac angiotensin-converting enzyme 2. Circulation. 2005;111(20):2605-2610. doi:10.1161/CIRCULATIONAHA.104.510461.

25. Ishiyama Y, Gallagher PE, Averill DB, Tallant EA, Brosnihan KB, Ferrario CM. Upregulation of angiotensin-converting enzyme 2 after myocardial infarction by blockade of angiotensin II receptors. Hypertension. 2004;43(5):970-976. doi:10.1161/01.HYP.0000124667.34651.1a.

26. Toni LS, Carroll IA, Jones KL, et al. Sequential analysis of myocardial gene expression with phenotypic change: Use of cross-platform concordance to strengthen biologic relevance

[published correction appears in PLoS One. 2019 Oct 22;14(10):e0224389]. PLoS One. 2019;14(8):e0221519. doi:10.1371/journal.pone.0221519.

27. Kao DP, Lowes BD, Gilbert EM, et al. Therapeutic Molecular Phenotype of beta-Blocker-Associated Reverse-Remodeling in Nonischemic Dilated Cardiomyopathy. Circ Cardiovasc Genet. 2015;8(2):270-283. doi:0.1161/CIRCGENETICS.114.000767.
28. Leary PJ, Kronmal RA, Bluemke DA, et al. Histamine H2 Receptor Polymorphisms, Myocardial Transcripts, and Heart Failure (from the Multi-Ethnic Study of Atherosclerosis and Beta-Blocker Effect on Remodeling and Gene Expression Trial). Am J Cardiol. 2018;121(2):256-261. doi:10.1016/j.amjcard.2017.10.016.
29. Sucharov CC, Kao DP, Port JD, et al. Myocardial microRNAs associated with reverse remodeling in human heart failure. JCI Insight. 2017;2(2):e89169. doi:10.1172/jci.insight.89169.
30. Peri-Okonny PA, Mi X, Khariton Y, Patel KK, et al. Target doses of heart failure medical therapy and blood pressure: Insights from the CHAMP-HF registry. JACC Heart Fail. 2019;7(4):350-358. doi:10.1016/j.jchf.2018.11.011.
31. Haga S, Yamamoto N, Nakai-Murakami C, et al. Modulation of TNF-alpha-converting enzyme by the spike protein of SARS-CoV and ACE2 induces TNF-alpha production and facilitates viral entry. Proc Natl Acad Sci U S A. 2008;105(22):7809-7814. doi:10.1073/pnas.0711241105.
32. Coutard B, Valle C, de Lamballerie X, Canard B, Seidah NG, Decroly E. The spike glycoprotein of the new coronavirus-2019-nCoV contains a furin-like cleavage site absent in CoV of the same clade. Antiviral Res. 2020;176:104742. doi:10.1016/j.antiviral.2020.104742.
33. Belouzard S, Chu VC, Whittaker GR. Activation of the SARS coronavirus spike protein via sequential proteolytic cleavage at two distinct sites. Proc Natl Acad Sci U S A. 2009;106(14):5871-5876. doi:10.1073/pnas.0809524106.

34. Lowes BD, Minobe WA, Abraham WT, et al**.** Changes in gene expression in the intact human heart: down-regulation of alpha-myosin heavy chain in hypertrophied, failing ventricular myocardium. J Clin Invest. 1997;100(9):2315-2324. doi:10.1172/JCI119770.

35. Lowes BD, Gilbert EM, Abraham WT, et al. Myocardial gene expression in dilated cardiomyopathy treated with beta-blocking agents. New Engl J Med. 2002;346(18):1357-1365. doi:10.1056/NEJMoa012630.

36. Dullens HFJ, Schipper MEI, van Kuik J, et al. Integrin expression during reverse remodeling in the myocardium of heart failure patients. Cardiovasc Pathol 2012;21(4):291-298. doi:10.1016/j.carpath.2011.09.009.

37. Okada H, Lai NC, Kawaraguchi Y, et al. Integrins protect cardiomyocytes from ischemia/reperfusion injury. J Clin Invest. 2013;123(10):4294-4308. doi:10.1172/JCI64216.

38. Martin FL, Chen HH, Cataliotti A, Burnett JC Jr. B-type natriuretic peptide: beyond a diagnostic. Heart Fail Clin. 2008;4(4):449-454. doi:10.1016/j.hfc.2008.03.011.

39 Santos RAS, Simoes e Silva AC, Maric C, et al. Angiotensin-(1-7) Is an endogenous ligand for the G protein-coupled receptor Mas. Proc Natl Acad Sci. 2003;100(14):8258-8263. doi: 10.1073/pnas.1432869100.

40. Tallant EA,, Ferrario CM, Gallagher PE. Angiotensin-(1–7) inhibits growth of cardiac myocytes through activation of the *mas* receptor. Am J Physiol Heart Circ Physiol. 2005;289:H1560–H1566. doi:10.1152/ajpheart.00941.2004.

41. Donoghue M, Hsieh F, Baronas E, et al. A novel angiotensin-converting enzyme-related carboxypeptidase (ACE2) converts angiotensin I to angiotensin 1-9. Circ Res. 2000;87(5):E1-9. doi:10.1161/01.res.87.5.e1.

42. Heald-Sargent T, Gallagher T. Ready, set, fuse! The coronavirus spike protein and acquisition of fusion competence. Viruses. 2012;4(4):557-580. doi:10.3390/v4040557.

43. Belouzard S, Millet JK, Licitra BN, Whittaker GR. Mechanisms of coronavirus cell entry mediated by the viral spike protein. Viruses. 2012;4(6):1011-1033. doi:10.3390/v4061011.
44. Takada Y, Ye X, Simon S. The integrins. Genome Biol. 2007;8(5):215. doi:10.1186/gb-2007-8-5-215.
45. Esfandiarei M, Suarez A, Amaral A, Si X, Rahmani M, Dedhar S, McManus BM. Novel role for integrin-linked kinase in modulation of coxsackievirus B3 replication and virus-induced cardiomyocyte injury. Circ Res. 2006;99(4):354-361. DOI: 10.1161/01.RES.0000237022.72726.01.
46. Legate KR, Fässler R. Mechanisms that regulate adaptor binding to beta-integrin cytoplasmic tails. J Cell Sci. 2009;122(Pt 2):187-198. doi: 10.1242/jcs.041624.
47. Xu Z, Shi L, Wang Y, et al. Pathological findings of COVID-19 associated with acute respiratory distress syndrome. Lancet Respir Med. 2020;8(4):420-422. doi:10.1016/S2213-2600(20)30076-X.
48. Tian S, Xiong Y, Liu H, Niu L, Guo J, Liao M, Xiao SY. Pathological study of the 2019 novel coronavirus disease (COVID-19) through postmortem core biopsies. Mod Pathol. 2020 Apr 14. doi: 10.1038/s41379-020-0536-x.
49. Tavazzi G, Pellegrini C, Maurelli M, et al. Myocardial localization of coronavirus in COVID-19 cardiogenic shock. Eur J Heart Fail. 2020 Apr 10. doi: 10.1002/ejhf.1828.
50. Tang Y, Nyengaard JR, Andersen JB, Baandrup U, Gundersen HJ. The application of stereological methods for estimating structural parameters in the human heart. Anat Rec. 2009;292(10):1630-1647. doi:10.1002/ar.20952.
51. Guo J, Wei Xiangxiang W, Li Q, et al. Single-cell RNA analysis on ACE2 expression provides insight into SARS-CoV-2 blood entry and heart injury. https://doi.org/10.1101/2020.03.31.20047621doi: medRxiv preprint (pre-peer review).

52. Zhang H, Penninger JM, Li Y, Zhong N, Slutsky AS. Angiotensin-converting enzyme 2 (ACE2) as a SARS-CoV-2 receptor: molecular mechanisms and potential therapeutic target. Intensive Care Med. 2020;46(4):586-590. doi:10.1007/s00134-020-05985-9.
53. Dales NA, Gould AE, Brown JA, et al. Substrate-based design of the first class of angiotensin-converting enzyme-related carboxypeptidase (ACE2) inhibitors. J Am Chem Soc. 2002;124(40):11852-11853.
54. Crackower MA, Sarao R, Oudit GY, et al. Angiotensin-converting enzyme 2 is an essential regulator of heart function. Nature. 2002;417(6891):822-828.
55. Hofmann H, Geier M, Marzi A, et al. Susceptibility to SARS coronavirus S protein-driven infection correlates with expression of angiotensin converting enzyme 2 and infection can be blocked by soluble receptor. Biochem Biophys Res Commun. 2004;319(4):1216-1221.
56. Qaradakhi T, Gadanec LK, McSweeney KR, et al. The potential actions of angiotensin-converting enzyme II (ACE2) activator diminazene aceturate (DIZE) in various diseases. Clin Exp Pharmacol Physiol. 2020;47:751-758.

TABLES

Table 1. Baseline characteristics, Number (%) or mean±SD

Characteristic	Nonfailing (NF), N=4	Failing/NDC (F/NDC), N=46	P value, NF vs. F/NDC	Failing/NDC Responders (R), N=30	Failing/NDC Nonresponders (NR), N= 16	P value, R vs. NR
Age	41.0±17.1	45.6±13.2	0.63	43.5±13.2	49.7±12.3	0.12
Gender	3M, 1F	33M,13F	0.94	21M, 9F	12M, 4F	0.72
Race, ethnicity	4W	30W,6B,7H,2A,1N	0.15	21W,4B,4H,1N	9W,2B,3H,1A,1N	0.35
Diabetes	0 (0)	8 (17)	0.36	5 (17)	3 (19)	0.86
Hypertension history	2 (50)	18 (39)	0.43	15 (50)	3 (19)	0.039
BSA (m2)	2.20±0.42	1.97±0.22	0.58	1.97±0.22	1.96±0.21	0.89
BMI (Kg/m2)	30.9±8.1	28.9±5.7	0.67	29.0±6.3	28.9±4.8	0.99
Creatine clearance (mg/dL)	87.7±7.9	80.2±22.5	0.18	85.3±18.8	71.0±26.2	0.066
HF failure duration (months)	–	23.9±45.9	–	7.0±10.0	55.7±67.0	0.011
Atrial fibrillation	1 (25)	10 (22)	0.88	4 (13)	6 (38)	0.058
NHYA class	2 I, 2 II	25 II, 21 III	0.87	16 II, 14 III	10 II, 6 III	0.55
Heart rate (bpm)	77±9	84±21	0.24	87±21	79±20	0.21
SBP (mmHg)	118±29	107±14	0.51	106±13	109±17	0.51
LVEF (%)	58.8±7.4	26.6±8.7	0.002	25.6±8.2	27.8±10.0	0.51
RVEF (%)	38.3±4.7	27.2±9.0	0.032	27.2±8.8	27.2±9.7	0.99
LV end diastolic volume (ml)	–	232±93	–	220±83	255±111	0.38
PWP mean, mmHg	7±6	12±8	0.12	11.3±8.7	14.5±7.7	0.21
PAP mean, mmHg	20±2	24±11	0.13	22.4±9.9	27.1±11.5	0.18
Cardiac index, L/min/m2	2.8±0.6	2.2±0.6	0.10	2.3±0.7	2.2±0.6	0.74
Mixed venous NE, pg/ml	372±152	492±331	0.44	452±267	574±438	0.39
Mixed venous BNP, pg/ml	90±46	234±234	0.035	203±240	334±200	0.21
ACEI, ARB doses (enalapril or losartan equivalents, mg)	ACEI N = 4 6.6±9.0 mg	ACEI N = 44 9.3±6,1 mg 1 ARB, 50 1 missing	ACEI, 0.59	ACEI, N = 27 8.8±5.0 mg ARB N = 3 46.9±38.7 mg	ACEI N = 14 8.2±5.0 mg ARB, N = 2 87.5±17.7 mg	ACEI, 0.75 ARB 0.15
β-blocker doses, mg/d (C = carvedilol, M = metoprolol succinate)	–	C, N=16, 75±24 M, N=30, 169±55	–	C, N=9, 78±23 M, N=21, 176±52	C, N=7, 71±27 M, N=9, 153±62	C, 0.63 M, 0.33

NF = Nonfailing group, F/NDC = Failing/Nonischemic Dilated Cardiomyopathy group; BSA = body surface area, BMI = body mass index; NYHA = New York Heart Association; LVEF, RVEF = left or right ventricular ejection fraction; PWP = mean pulmonary wedge pressure; PAP = mean pulmonary artery pressure; ACEI = angiotensin converting enzyme inhibitor, ARB = angiotensin receptor blocker; W = White, B = Black, H = Hispanic, A = Asian, N = Native American.

Table 2. Change from baseline data, microarray and RNA-Seq

Gene	Microarray						RNA-Seq						Level of Evidence* remodeling association
	R		NR		R vs. NR		R		NR		R vs. NR		
	FC	P value	FC	P value	FC	P value	FC	P value	FC	P value	FC	P value	
RAS													
ACE2	0.675	<0.0001	1.144	0.60	0.591	0.0006	0.402	0.031	1.216	0.69	0.331	0.004	UE
ACE	1.040	0.65	1.02	0.67	1.016	0.95	1.065	0.69	1.087	0.44	0.980	0.44	NE
AGT	1.049	0.32	1.078	0.30	0.97	0.76	0.924	0.44	1.049	1.00	0.973	0.18	NE
AGTR1	1.479	0.003	1.253	0.13	1.181	0.44	1.814	0.031	1.404	0.031	1.293	0.18	PE
AGTR2	0.964	0.21	1.181	0.23	0.816	0.060	0.900	0.31	1.703	0.44	0.528	0.24	NE
Proteases													
TMPRSS2	1.000	0.84	1.000	0.63	1.000	0.62	Transcript not detected						NE
TMPRSS11D	0.943	0.044	1.017	0.99	0.928	0.23	0.977	1.00	2.149	0.59	0.452	0.84	NE
CTSL1	1.180	0.006	1.085	0.013	0.918	0.92	1.100	0.16	0.999	0.69	1.101	0.18	NE
ADAM17	1.018	0.56	1.025	0.67	0.993	0.92	0.865	0.094	1.042	0.44	0.830	0.65	NE
FURIN	1.043	0.82	0.952	0.22	1.10	0.55	0.912	0.31	9.938	0.31	0.972	0.48	NE
Remodeling													
NPPB	0.522	<0.0001	1.783	0.38	0.295	0.0015	0.078	0.031	1.404	0.84	0.055	0.009	UE
MYH6	1.171	0.052	0.821	0.002	1.426	0.0002	2.426	0.062	0.885	0.56	2.742	0.015	E
ATP2A2	1.050	0.077	0.989	0.60	1.062	0.056	1.388	0.031	1.005	1.00	1.044	0.31	PE
PLN	1.108	0.001	0.986	0.43	1.123	0.006	1.281	0.22	1.034	0.44	1.239	0.24	E
ADRB1	1.335	0.001	1.124	0.53	1.187	0.16	1.596	0.031	1.084	0.84	1.473	0.041	E
Reference													
GAPDH	1.026	0.99	0.983	0.30	1.044	0.69	0.994	0.84	1.071	0.44	0.928	0.48	NE

FC = Fold change, calculated from mean values as described in Methods; P values are calculated by Wilcoxon rank sum of mRNA readouts as described in Methods. Level of evidence of remodeling association is as described in the Supplement, Table S2. *UE = *Unequivocal Evidence*, E = *Evidence*, PE = *Possible Evidence*, NE = *No Evidence*. R =LVEF Responders, NR = Nonresponders; FC = Log2 fold change, values <1.0 are a decrease in expression, >1.0 an increase. TMPRSS2 = transmembrane serine protease 2, CTSL1 = cathepsin L, TMPRSS11D = trypsin-like protease (HAT), ADAM17 = ADAM metallopeptidase domain 17 (also known as TACE, TNFα converting enzyme); FURIN = Furin, paired basic amino acid cleaving enzyme (also known as PACE). GAPDH baseline NF and F/NDC were respectively 13.45±0.08 and 13.40±0.13 fluorescence units, P = 0.69.

Table 3. Analysis of baseline and serial/reverse remodeling Integrins gene expression data

Gene	Baseline mRNA Expression (Array Fluorescence Units)				Array Change from Baseline						RNA-Seq Change from Baseline						Level of Evidence,* remodeling association
					R		NR		R vs. NR		R		NR		R vs. NR		
	NF	F/ NDC	FD, F/NF	P value	FC	P value	FC	P value	FC	P value	FC	P value	FC	P value	FC	P value	
ACE2 Binding, Virus Internalization																	
ITGB1†	8.09 ±0.05	7.90 ±0.23	0.88	0.13	0.973	0.18	1.020	0.82	0.954	0.29	0.769	0.031	1.055	0.44	0.729	0.15	NE
ITGA2	5.16 ±0.86	5.40 ±0.57	1.18	0.46	1.273	0.15	1.082	0.60	1.198	0.52	1.595	0.22	1.069	0.84	1.492	0.31	NE
ACE2 Binding, Virus Internalization, LV Remodeling																	
ITGA5†	10.14 ±0.21	10.49 ±0.37	1.28	0.039	0.880	0.004	1.001	0.53	0.880	0.11	0.827	0.16	0.953	0.84	0.867	0.48	E
Virus Internalization																	
ITGB3†	3.84 ±0.04	4.00 ±0.16	1.11	0.026	0.944	0.015	1.080	0.034	0.873	0.0007	Transcript not detected						E
ITGA4	3.50 ±0.05	3.73 ±0.22	1.18	0.030	0.985	0.73	1.032	0.98	0.954	0.74	1.188	0.84	1.176	0.44	1.010	1.00	PE
ITGA9	7.20 ±0.13	7.27 ±0.14	1.05	0.39	0.970	0.13	0.992	0.74	0.978	0.58	1.016	0.69	1.029	0.56	0.988	0.82	NE
ITGAV†	11.91 ±0.13	11.95 ±0.13	1.03	0.60	0.979	0.56	0.977	0.32	1.002	0.95	0.670	0.031	0.961	1.00	0.698	0.009	PE
Virus Internalization, LV Remodeling																	
ITGA6	7.86 ±0.03	7.58 ±0.21	0.83	0.009	1.033	0.67	0.988	0.98	1.046	0.43	1.019	1.00	1.154	0.22	0.883	0.39	PE
ITGB6†	5.62 ±0.39	5.11 0.25	0.70	0.034	1.292	<0.0001	1.070	0.53	1.208	0.002	1.295	0.44	1.020	0.56	1.270	0.39	E
Laminin Binding, LV Remodeling																	
ITGA7	9.75 ±0.18	10.07 ±0.24	1.24	0.044	0.913	0.015	1.032	0.53	0.885	0.026	0.749	0.031	1.013	0.84	0.740	0.065	UE

See Table 2 and Methods for description of how Fold Change (FC) or Fold Difference (FD are calculated, based on log base2 transformation. P values are from Wilcoxon rank sum tests of NF vs. F/NDC microarray (array) fluorescence intensity or Wilcoxon signed rank tests of baseline vs. 3 or 12 month LOCF values (Change from Baseline). *UE = *Unequivocal Evidence*, E = *Evidence*,

PE = *Possible Evidence*, NE = *No Evidence*. †When dimerized contains binding motif for an RGD (arginine-glycine aspartic acid) sequence, a domain contained in the CoV-2 spike protein and in other viruses.

FIGURE LEGENDS

Figure 1. Left (LVEF) and right ventricular ejection fraction (RVEF) data. A. At baseline in Nonfailing controls (NF) and in nonischemic dilated cardiomyopathy patients with heart failure (F/NDC); B. F/NDC patients who were treated for 3 or 12 months with beta-blocking agents to effect reverse remodeling in N = 30 (Responders, R) and N = 16 (Nonresponders, NR). LVEF and RVEF are in absolute %. Data are plotted as baseline values, last observation carried forward (LOCF, N = 8 at 3 months, 38 at 12 months) and the LOCF-BsL difference calculated for each patient and averaged.

Figure 2. Renin-angiotensin (RAS) and protease mRNA expression, by microarray in fluorescence units (a logarithmic signal) ±SD. NF = 4 nonfailing controls, F/NDC = 46 nonischemic dilated cardiomyopathy heart failure patients (F/NDC), ACE2 = angiotensin converting enzyme 2, ACE = angiotensin converting enzyme, AGT = angiotensinogen, TMPRSS2 = transmembrane serine protease 2, CTSL1 = cathepsin L, TMPRSS11D = trypsin-like protease (HAT), ADAM17 = metallopeptidase domain 17, FURIN = furin.

Figure 3. mRNA expression of genes associated with remodeling see Figure 2 for further description. NPPB = B type natriuretic peptide, MYH6 = myosin heavy chain 6 (also known as α-myosin heavy chain), ATP2A2 = sarcoplasmic reticulum Ca^{2+} ATPase, PLN = phospholamban, ADRB1 = β_1-adrenergic receptor, AGTR1 = angiotensin type 1 receptor, AGTR2 = angiotensin type 2 receptor.

Figure 4. Position of angiotensin converting enzyme 2 (ACE2) within the renin-angiotensin-aldosterone system. Substrate or effector molecules are in italics, enzymes are within ovals, receptors (R) are bolded and shadowed text, and inhibitors are underlined. MRA =

mineralocorticoid receptor antagonist, NEP = neutral endopeptidase, ACE = angiotensin converting enzyme, MASR = MAS1 (also known as MAS) receptor.

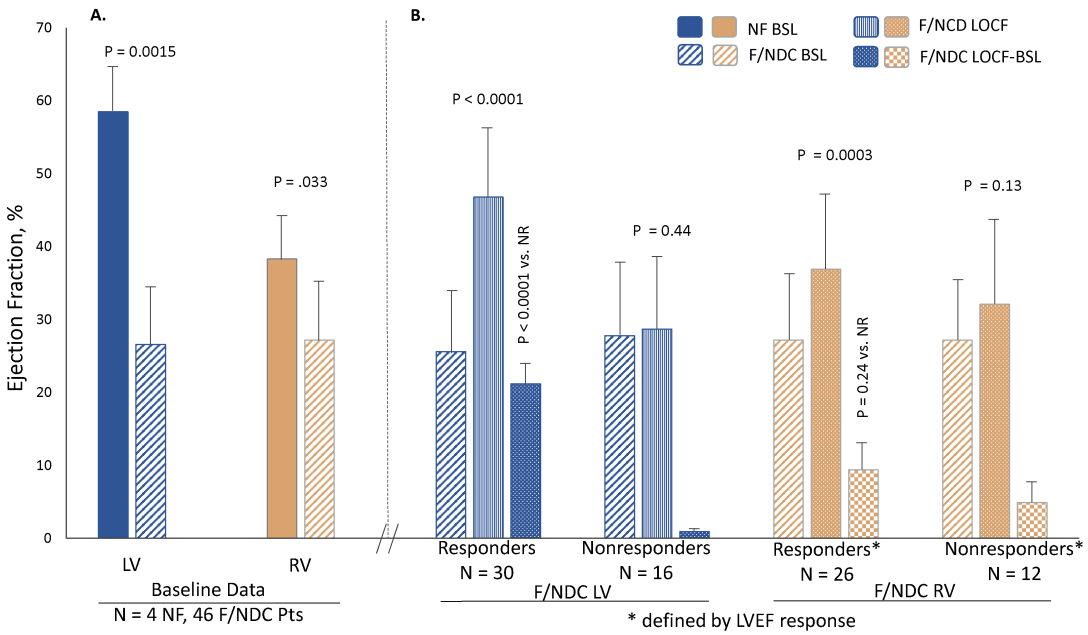
A.
B.
NF BSL
F/NDC BSL
F/NCD LOCF
F/NDC LOCF-BSL
Ejection Fraction, %
70
60
50
40
30
20
10
0
P = 0.0015
P = .033
P < 0.0001
P < 0.0001 vs. NR
P = 0.44
P = 0.0003
P = 0.24 vs. NR
P = 0.13
LV
RV
Responders
N = 30
Nonresponders
N = 16
Responders*
N = 26
Nonresponders*
N = 12
Baseline Data
N = 4 NF, 46 F/NDC Pts
F/NDC LV
F/NDC RV
* defined by LVEF response

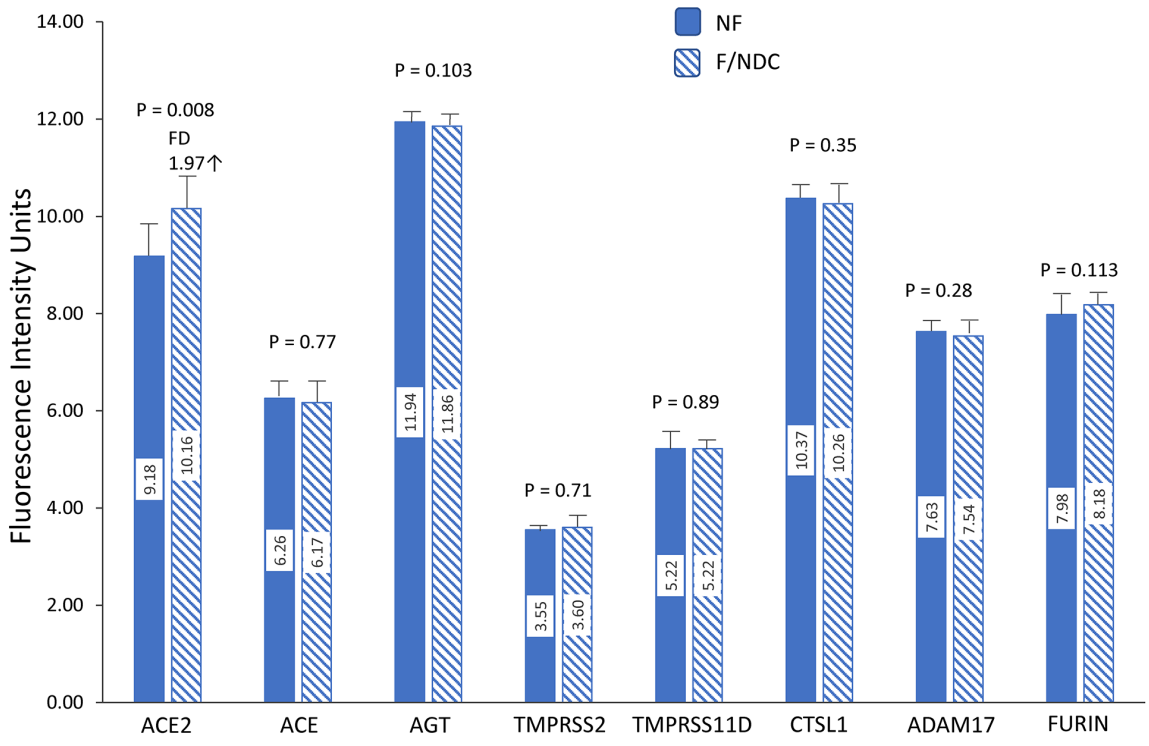
NF
F/NDC
Fluorescence Intensity Units
14.00
12.00
10.00
8.00
6.00
4.00
2.00
0.00
P = 0.008
FD
1.97↑
P = 0.77
P = 0.103
P = 0.71
P = 0.89
P = 0.35
P = 0.28
P = 0.113
9.18
10.16
6.26
6.17
11.94
11.86
3.55
3.60
5.22
5.22
10.37
10.26
7.63
7.54
7.98
8.18
ACE2
ACE
AGT
TMPRSS2
TMPRSS11D
CTSL1
ADAM17
FURIN

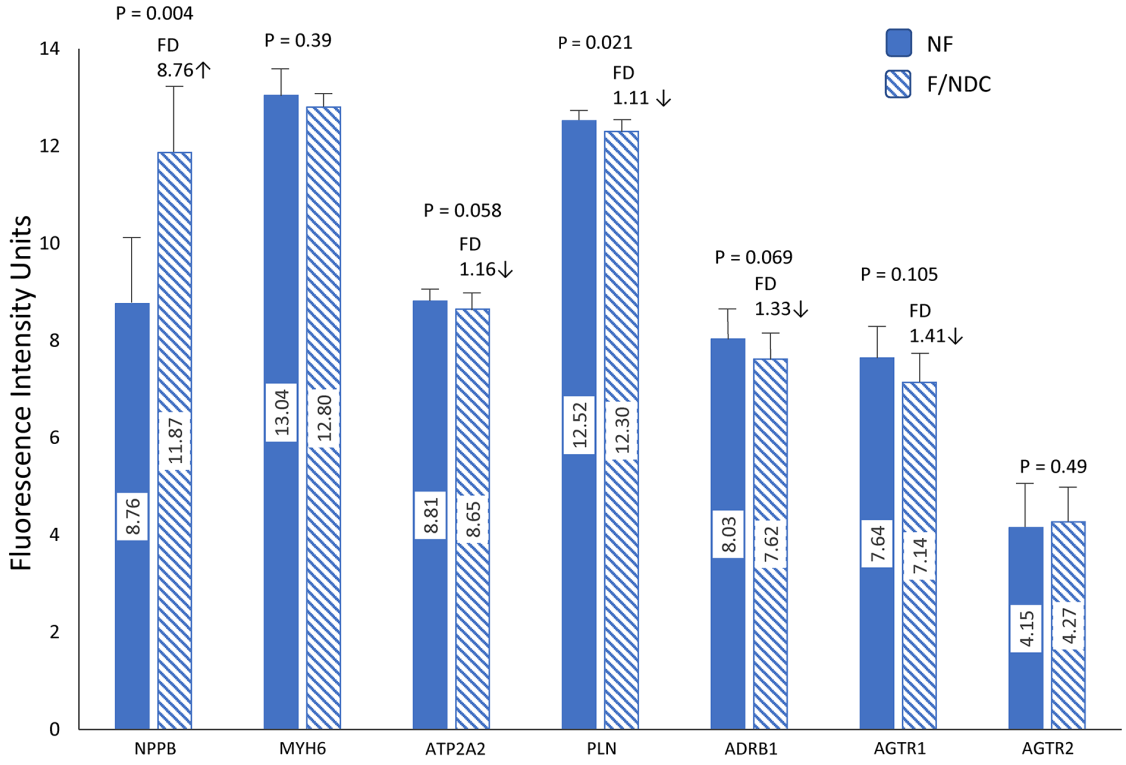
P = 0.004
FD
8.76↑
P = 0.39
P = 0.021
FD
1.11 ↓
P = 0.058
FD
1.16↓
P = 0.069
FD
1.33↓
P = 0.105
FD
1.41↓
P = 0.49
NF
F/NDC
Fluorescence Intensity Units
0
2
4
6
8
10
12
14
8.76
11.87
13.04
12.80
8.81
8.65
12.52
12.30
8.03
7.62
7.64
7.14
4.15
4.27
NPPB
MYH6
ATP2A2
PLN
ADRB1
AGTR1
AGTR2